第 31 卷第 2 期 无 机 化 学 学 报 Vol.31 No.2
2015 年 2 月 CHINESE JOURNAL OF INORGANIC CHEMISTRY 420-428

两个基于 4-咪唑羧酸配体超分子配位聚合物的合成、结构和性质

陈水生*,[1,2] 吕弹龙[1] 乔 瑞[1] 朱娟娟[1] 盛良全[1]
([1]阜阳师范学院化学与材料工程学院,阜阳 236041)
([2]南京大学配位化学国家重点实验室,南京 210093)

摘要:以含 4-咪唑和羧酸基团的双功能基团 4-咪唑基苯甲酸(HL_1)为配体,用水热法合成了 2 个超分子化合物[$Cd(L_1)(HL_1)I$] (**1**)和[$Co_2(L_1)_4(H_2O)_8$] (**2**),并进行了元素分析、红外、热重、粉末衍射及 X-射线单晶衍射等表征。晶体结构解析结果表明:配合物 **1** 属于单斜晶系,$P2_1/c$ 空间群,L_1^-配体连接 Cd(Ⅱ)离子成一维链,这些一维链通过氢键连接成三重贯穿的 α-Po 结构的超分子聚合物;配合物 **2** 不对称结构单元中,存在 3 种不同的金属 Co(Ⅱ)中心单核分子,这些相互独立的分子单元通过丰富的氢键连接成三维的聚合物。同时,对配合物 **1** 室温下的固体荧光性质和配合物 **2** 对气体的吸附性能进行了研究。

关键词:合成;超分子聚合物;荧光性质;气体吸附性质
中图分类号:O614.24+2;O614.81+2 **文献标识码**:A **文章编号**:1001-4861(2015)02-0420-09
DOI:10.11862/CJIC.2015.025

Syntheses, Structures and Properties of Two Supramolecular Polymers Constructed from 4Imidazole Carboxylate Ligand

CHEN Shui-Sheng*,[1,2] LÜ Dan-Long[1] QIAO Rui[1] ZHU Juan-Juan[1] SHENG Liang-Quan[1]
([1]*College of Chemistry & Chemical Engineering, Fuyang Normal College, Fuyang, Anhui* 236041, *China*)
([2]*State Key Laboratory of Coordination Chemistry, Nanjing University, Nanjing* 210093, *China*)

Abstract: Two complexes, [$Cd(L_1)(HL_1)I$] (**1**, HL_1=4-(1H-imidazol-4-yl)benzoic acid) and [$Co_2(L_1)_4(H_2O)_8$] (**2**), have been hydrothermally prepared and characterized by single-crystal X-ray diffraction, elemental analysis, IR spectroscopy, photoluminescence property, TG and PXRD. Complex **1** crystallizes in monoclinic, space group $P2_1/c$. The L_1^- ligands link Cd(Ⅱ) atoms to form one-dimensional chains, which are further bridged to form a three-dimensional three-fold interpenetrating α-Po supramolecular polymer by hydrogen bonds. X-ray diffraction analysis revealed three different kinds of Co(Ⅱ) centre mononuclear molecules in the asymmetric unit. The independent mononuclear units are bridged to form a three-dimensional supramolecular polymer by extensive hydrogen bonds interactions. Solid state luminescent property of **1** and sorption property of **2** have been investigated. CCDC: 983657, **1**; 1027672, **2**.

Key words: synthesis; supramolecular polymer; photoluminescence property; sorption property

The fabrication of functional metal-organic frameworks (MOFs), are totally dependent on the judicious choice of appropriate organic spaces with different binding sites, lengths, and directions[1], and reaction conditions have a great influence on the structures of the resulting complexes[2]. In this regard,

收稿日期:2014-10-07。收修改稿日期:2014-10-14。
国家自然科学基金(No.21171040, 21302019)、南京大学配位化学重点实验室开放基金、国家大学生创新项目(No.201310371004)和有机教研项目(No.2013JCJS01) 资助项目。
*通讯联系人。E-mail:chenss@fync.edu.cn

organic linkers with N and/or O donors have been often employed as effective building blocks in the construction of MOFs[3]. Among them, a series of polyfunctional organic linkers combining anionic carboxylates and nitrogen donors such as 4-(1*H*-imidazol-1-yl)benzoic acid, 3,5-di(imidazol-1-yl)benzoic acid and 5-(4*H*-1,2,4-triazol-4-yl)benzene-1,3-dicarboxylic acid have been developed in our previous study, which possess more tunable factors to be employed as good candidates for the construction of novel MOFs[4-6]. In additional, the intermolecular non-covalent bonding interactions including hydrogen bonds[7], $\pi\cdots\pi$ stacking[8] and C–H$\cdots\pi$[9] are also important factors in the construction of supramolecular frameworks. Taking the favorable coordination ability of N/O-donor difunctional groups into account, the 1H-imidazol-4-yl group and carboxylate groups-containing ligand (HL_1) was employed in this study. It is obvious that the HL_1 ligand possesses favorable coordination ability due to the carboxylate and 1*H*-imidazol-4-yl groups; moreover, the NH, N and O atoms of the difunctional groups can act as hydrogen bonding donor or acceptor, contributing to the construction of supramolecular structures [10]. In this paper, we report the synthesis and crystal structure of two supramolecular polymers built from hydrogen bonding interactions.

1　Experimental

1.1　Materials and measurements

All the commercially available chemicals and solvents were of reagent grade and used as received without further purification. The ligand HL_1 was synthesized according to our previously reported literature[11]. Elemental analyses were performed on a Perkin-Elmer 240C Elemental Analyzer. IR spectra were recorded on a Bruker Vector 22 FT-IR spectrophotometer using KBr pellets. Thermogravimetric analyses (TGA) were performed on a simultaneous SDT 2960 thermal analyzer under nitrogen at a heating rate of 10 ℃·min^{-1}. Powder X-ray diffraction (PXRD) patterns were measured on a Shimadzu XRD-6000 X-ray diffractometer with Cu $K\alpha$ (λ=0.154 18 nm) radiation at room temperature. The luminescence spectra for the powdered solid samples at room temperature were measured on an Aminco Bowman Series 2 spectrofluorometer with a xenon arc lamp as the light source. In the measurements of emission and excitation spectra the pass width is 5 nm, and all the measurements were carried out under the same experimental conditions. Nitrogen (N_2) and water (H_2O) sorption experiments were carried out on an Autosorb-iQ gas sorption instrument in Quantachrome Instruments U.S. The sample was activated by using the "outgas" function of the surface area analyzer for 24 hours at 180 ℃.

1.2　Synthesis of complex [Cd(L_1)(HL_1)I] (1)

A mixture of HL_1 (0.018 8 g, 0.1 mmol) and CdI_2 (0.036 6 g, 0.1 mmol) in 10 mL H_2O was sealed in a 16 mL Teflon-lined stainless steel container and heated at 140 ℃ for 3 d. Colorless needle crystals of **1** were collected with a yield of 72% by filtration and washed with water and ethanol for several times. Anal. Calcd.(%) for $C_{20}H_{15}N_4O_4ICd$: C, 39.08; H, 2.46; N, 9.11. Found (%): C, 38.73; H, 2.39; N, 9.21. IR(KBr, cm^{-1}): 3 511~2 639(m), 1 705(m), 1 632(m), 1 606(s), 1 584 (m), 1 532 (s), 1 510 (s), 1 411 (vs), 1 306(w), 1 198(m), 1 124(m), 964(w), 864(s), 838(m), 782(s), 716(m), 703(w), 6258(m), 508(m).

1.3　Synthesis of complex [$Co_2(L_1)_4(H_2O)_8$] (2)

Complex **2** was obtained by the same procedure used for preparation of **1** except that the metal salt was replaced by $Co(NO_3)_2\cdot 6H_2O$ (29.1 mg, 0.1 mmol). Yellow block crystals of **2** were collected in 83% yield. Anal. Calcd.(%) for $C_{20}H_{22}N_4O_8Co$: C, 47.53; H, 4.39; N, 11.09. Found (%): C, 47.13; H, 4.51; N, 11.14. IR(KBr, cm^{-1}): 3 650~2 530(m), 1 604(s), 1 586 (s), 1 521(vs), 1 462(m), 1408(vs), 1372(vs), 1173(m), 1152 (m), 1098 (m), 965 (w), 851 (s), 832 (s), 785 (s), 6547(w), 631(w), 528(w), 504(w).

1.4　Crystal structure determination

The X-ray diffraction measurements for **1** and **2** were performed on Bruker Smart Apex CCD diffractometer with graphite-monochromated Mo $K\alpha$ radiation (λ=0.071 075 nm) at room temperature. The structures of complexes were solved by direct methods, and the

non-hydrogen atoms were located from the trial structure and then refined anisotropically with SHELXTL using a full-matrix least-squares procedure based on F^2 values[12]. All non-hydrogen atoms were refined anisotropically. All the hydrogen atoms except for those of water molecules were generated geometrically and refined isotropically using the riding model. The hydrogen atoms of the water molecules in **2** were located in a difference Fourier map. Details of the crystal parameters, data collection and refinements for **1** and **2** are summarized in Table 1. Selected bond lengths and angles for **1** and **2** are listed in Table 2.

CCDC: 983657, **1**; 1027672, **2**.

Table 1 Crystallographic data of complexes 1 and 2

Complex	**1**	**2**
Empirical formula	$C_{20}H_{15}N_4O_4ICd$	$C_{20}H_{22}N_4O_8Co$
Formula weight	614.66	505.35
Crystal system	Monoclinic	Monoclinic
Space group	$P2_1/c$	$P2_1/c$
a / nm	0.892 25(5)	2.229 5(10)
b / nm	2.725 72(16)	0.743 3(3)
c / nm	0.869 57(6)	2.508 8(11)
β / (°)	105.780 0(10)	90.000(5)
V / nm^3	2.035 1(2)	4.157(3)
Z	4	8
θ range / (°)	1.69~25.00	1.82~25.00
Absorption coefficient / mm^{-1}	2.625	0.884
F(000)	1 184	2 088
Reflections collected / unique	13 758 / 4 685 (R_{int}=0.023 4)	29 059 / 7 278 (R_{int}=0.053 7)
Data / restraints / parameters	4 685 / 0 / 272	7 278 / 0 / 637
Final R indices [$I>2\sigma(I)$]	R=0.034 0, wR=0.110 2	R=0.040 3, wR=0.121 3
Largest diff. peak and hole / (e·nm^{-3})	783 and −1 607	463 and −922

Table 2 Selected bond lengths (nm) and bond angles (°) of complexes 1 and 2

		1			
Cd(1)-N(3)	0.222 4(3)	Cd(1)-N(1)^i	0.223 8(3)	Cd(1)-I(1)	0.269 7(5)
Cd(1)-O(2)	0.223 6(3)	Cd(1)-O(1)	0.277 3(3)		
N(3)-Cd(1)-O(2)	125.88(12)	N(3)-Cd(1)-N(1)^i	112.89(11)	O(2)-Cd(1)-N(1)^i	86.80(10)
N(3)-Cd(1)-I(1)	111.19(9)	O(2)-Cd(1)-I(1)	106.61(9)	N(1)^i-Cd(1)-I(1)	110.95(10)
		2			
Co(1)-O(10)	0.207 5(19)	Co(1)-O(12)	0.208 6(2)	Co(1)-O(11)	0.209 9(2)
Co(1)-O(9)	0.211 4(2)	Co(1)-N(5)	0.213 0(2)	Co(1)-N(3)	0.214 5(2)
Co(2)-O(3)	0.207 0(19)	Co(2)-O(4)^i	0.210 6(2)	Co(2)-N(1)	0.211 8(2)
Co(3)-N(7)	0.210 3(3)	Co(3)-O(15)	0.210 9(2)	Co(3)-O(16)	0.212 74(19)
O(10)-Co(1)-O(12)	175.47(8)	O(10)-Co(1)-O(11)	86.61(8)	O(12)-Co(1)-O(11)	94.90(8)
O(10)-Co(1)-O(9)	87.31(9)	O(12)-Co(1)-O(9)	91.45(9)	O(11)-Co(1)-O(9)	172.84(9)
O(10)-Co(1)-N(5)	92.10(9)	O(12)-Co(1)-N(5)	92.17(9)	O(11)-Co(1)-N(5)	90.21(8)
O(9)-Co(1)-N(5)	86.22(8)	O(10)-Co(1)-N(3)	88.33(9)	O(12)-Co(1)-N(3)	87.34(9)
O(11)-Co(1)-N(3)	92.46(8)	O(9)-Co(1)-N(3)	91.14(8)	N(5)-Co(1)-N(3)	177.31(8)
O(3)^i-Co(2)-O(3)	180.00(11)	O(3)^i-Co(2)-O(4)	90.22(9)	O(3)-Co(2)-O(4)	89.78(9)

Continued Table 2

O(3)-Co(2)-O(4)^{i}	90.22(9)	O(4)-Co(2)-O(4)^{i}	180.00(16)	O(3)^{i}-Co(2)-N(1)	92.80(9)
O(3)-Co(2)-N(1)	87.20(9)	O(4)-Co(2)-N(1)	86.63(8)	O(4)^{i}-Co(2)-N(1)	93.37(8)
N(1)-Co(2)-N(1)^{i}	180.00(13)	N(7)-Co(3)-N(7)^{ii}	180.00(1)	N(7)-Co(3)-O(15)	90.56(8)
N(7)^{ii}-Co(3)-O(15)	89.44(8)	N(7)-Co(3)-O(16)	91.20(9)	O(15)-Co(3)-O(16)	90.10(8)
N(7)-Co(3)-O(16)^{ii}	88.80(9)	O(15)-Co(3)-O(16)^{ii}	89.90(8)	O(16)-Co(3)-O(16)^{ii}	180.00(5)

Symmetry codes: ^{i} x+1, −y+3/2, z−1/2 for **1**; ^{i} −x, −y, −z; ^{ii} −x+1, −y+1, −z+1 for **2**

2　Results and discussion

2.1　Crystal structure of 1

Single-crystal X-ray diffraction analysis revealed that complex **1** crystallizes in the monoclinic system with space group $P2_1/c$. As shown in Fig.1, there are one crystallographically unique Cd (Ⅱ) ions, one coordinated I^- anion, one deprotonated L_1^- and one HL_1 ligand in the asymmetric unit. The central Cd1 ion is five-coordinated by two oxygen (O1, O2) atoms of chelating carboxylate groups from L_1^- ligand and N3, N1A atoms from two distinct HL_1 and L_1^- ligand respectively, and a coordinated I^-, with Cd1-O bond distances being 0.223 6(3) and 0.277 3(3) nm, and Cd1-N ones of 0.222 4(3) and 0.223 8(3) nm (Table 2). A distance of 0.277 3(3) nm between Cd1 and O1 indicates the existence of weak interaction between them[13]. The bond angles around the cadmium ion range from 86.80(10)° to 125.88(12)° (Table 2). The L_1^- ligands link Cd(Ⅱ) atoms using its carboxylate groups in μ_1-η^1:η^1-chelating mode to form a one-dimensional (1D) chain, while the undeprotonated terminated ligand HL_1 use nitrogen atoms to coordinated with Cd(Ⅱ) ions (Fig.2). Significantly, the carboxylate moieties and N/NH groups serving as a hydrogen bonding acceptor/donor can effectively benefit the construction of supramolecular structures. As a result, abundant hydrogen bonds are present between these groups, as exhibited in Table 3. The 1D chains are linked together by this set of non-covalent forces like N−H⋯O, O−H⋯O, C−H⋯O hydrogen bonding interactions (N(2)⋯O(3)^{i} 0.277 8(4) nm, N(2)−H(2A)⋯O(3)^{i} 167°; N(4)⋯O(1)^{iii} 0.283 8(4) nm, N(4)−H(4B)⋯O(1)^{iii} 162°; O(4)⋯O(1)^{ii} 0.266 7(4) nm, O(4)−H(4A)⋯O(1)^{ii} 176°; C(9)⋯O(2)^{iv} 0.266 7(4) nm, C(9)−H(9)⋯O(2)^{iv} 119°; C(19)⋯O(4)^{v} 0.303 0(5) nm C(19)−H(19)⋯O(4)^{v} 135°) to give a three-dimensional (3D) framework (Fig.3). Examining the 3D framework carefully, we can find that hydrogen bonds link the adjacent two Cd(Ⅱ) ions into binuclear units as shown in Fig.4. Each binuclear Cd(Ⅱ) units

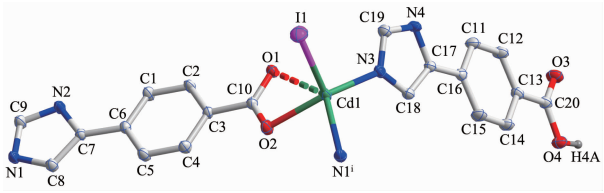

Symmetry code: ^{i} 1+x, 3/2−y, −1/2+z

Fig.1　View of the coordination environment of Cd(Ⅱ) atom with thermal ellipsoids drawn at the 30% probability level for the complex **1**

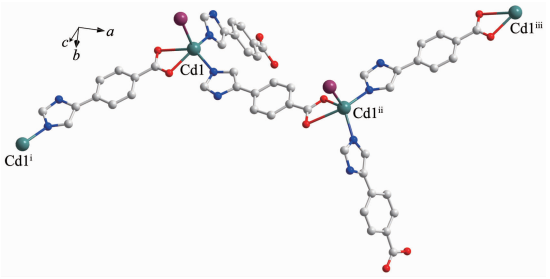

Symmetry code: ^{i} −1+x, 3/2−y, −1/2+z; ^{ii} 1+x, 3/2−y, −1/2+z; ^{iii} 2+x, y, −1+z

Fig.2 1D chain structure of **1**

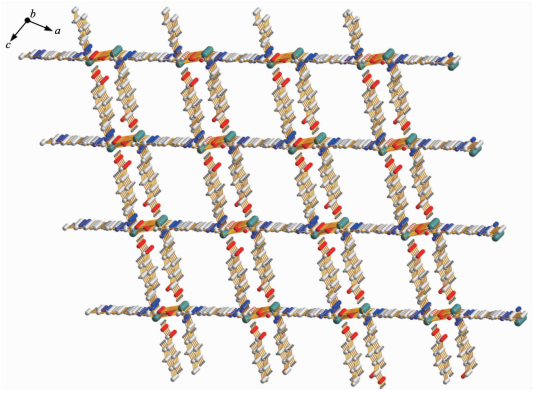

Fig.3　3D supramolecular framework of **1** built by the hydrogen bonds

Table 3 Distances (nm) and angles (°) of hydrogen bonding for complexes 1 and 2

D–H···A	*d*(D-H)	*d*(H···A)	*d*(D···A)	∠(D–H–A)
1				
N(2)–H(2A)···O(3)^{i}	0.086 0	0.193 0	0.277 8(4)	167
O(4)–H(4A)···O(1)^{ii}	0.082 0	0.186 0	0.266 7(4)	170
N(4)–H(4B)···O(1)^{iii}	0.086 0	0.201 0	0.283 8(4)	162
C(9)–H(9)···O(2)^{iv}	0.093 0	0.247 0	0.303 0(5)	119
C(19)–H(19)···O(4)^{v}	0.093 0	0.251 0	0.323 4(5)	135
2				
N(2)–H(2A)···O(7)^{i}	0.086 0	0.219 0	0.294 2(3)	145.00
O(3)–H(3)···O(5)^{ii}	0.082 0	0.187 0	0.261 9(3)	151.00
O(3)–H(3B)···O(1)^{iii}	0.087(3)	0.184(3)	0.270 3(3)	173(3)
O(4)–H(4B)···O(2)^{iv}	0.070(4)	0.209(4)	0.278 1(3)	169(4)
O(4)–H(4C)···O(2)^{iii}	0.079 0	0.210 0	0.286 3(3)	161.00
N(6)–H(6)···O(14)^{v}	0.086 0	0.204 0	0.279 2(3)	146.00
O(9)–H(9A)···O(5)^{iv}	0.082 0	0.243 0	0.306 1(3)	134.00
O(9)–H(9A)···O(6)^{iv}	0.082 0	0.219 0	0.298 8(3)	163.00
O(9)–H(9B)···O(7)^{i}	0.081(5)	0.209(5)	0.284 7(3)	155(5)
O(10)–H(10)···O(13)	0.082 0	0.189 0	0.262 4(3)	149.00
O(10)–H(10A)···O(8)^{vi}	0.084(4)	0.188(4)	0.271 2(3)	172(3)
O(11)–H(11A)···O(6)^{vii}	0.082 0	0.205 0	0.283 4(3)	160.00
O(11)–H(11B)···O(7)^{vi}	0.089(5)	0.190(5)	0.278 1(3)	172(4)
O(12)–H(12A)···O(1)^{iv}	0.082 0	0.203 0	0.272 4(3)	142.00
O(12)–H(12B)···O(5)^{iv}	0.082(4)	0.191(4)	0.270 6(3)	162(3)
O(15)–H(15A)···O(13)^{viii}	0.082 0	0.260 0	0.224 6(3)	137.00
O(15)–H(15A)···O(14)^{viii}	0.082 0	0.204 0	0.284 4(3)	165.00
O(15)–H(15B)···O(14)^{vi}	0.086(4)	0.208(4)	0.287 2(3)	153(3)
O(16)–H(16)···O(8)^{v}	0.082 0	0.207 0	0.277 7(3)	145.00
O(16)–H(16B)···O(13)^{viii}	0.090(3)	0.178(3)	0.266 9(3)	174(2)
C(9)–H(9)···O(11)^{ix}	0.093 0	0.254 0	0.227 7(4)	137.00
C(39)–H(39)···O(6)	0.093 0	0.247 0	0.327 7(4)	123.00

Symmetry nodes: ^{i} $-x$, $1-y$, $2-z$; ^{ii} $1-x$, $1-y$, $2-z$; ^{iii} $-x$, $1-y$, $1-z$; ^{iv} $-1+x$, $3/2-y$, $1/2+z$; ^{v} $-1+x$, y, $-1+z$ for **1**; ^{i} x, $1/2-y$, $1/2+z$; ^{ii} $-x$, $-1/2+y$, $1/2-z$; ^{iii} $-x$, $1/2+y$, $1/2-z$; ^{iv} x, $1/2-y$, $-1/2+z$; ^{v} $1-x$, $1-y$, $-z$; ^{vi} x, $3/2-y$, $1/2+z$; ^{vii} x, $3/2-y$, $-1/2+z$; ^{viii} $1-x$, $1/2+y$, $1/2-z$; ^{ix} x, $-1+y$, z for **2**

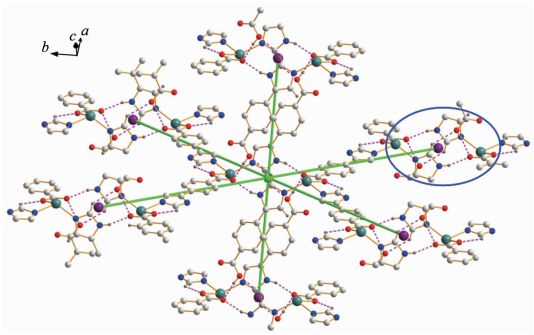

Hydrogen bonds indicated by dashed line

Fig.4 View of the linkages of a binuclear Cd(Ⅱ) nodes with six adjacent identical cores of **1**

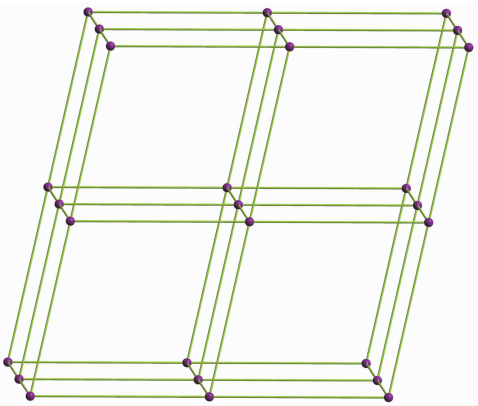

Fig.5 Schematic representation of 3D α-Po net of **1**

links six identical motifs through L_1^- ligands leading to formation of a 3D uninodal network with $(4^{12}\cdot6^3)$ α-Po topology by taking the binuclear motifs as 6-connecting nodes and the L_1^- ligands as linkers (Fig.5)[14]. Apparently, the 3D net exist large channels along the b axis, and the large vacancy of the α-Po net facilitates the interpenetration. Of particular interest, the most striking feature of complex **1** is that three identical 3D nets are interlocked each other, leading to the formation of a three-fold interpenetrated 3D to 3D architecture (Fig.6).

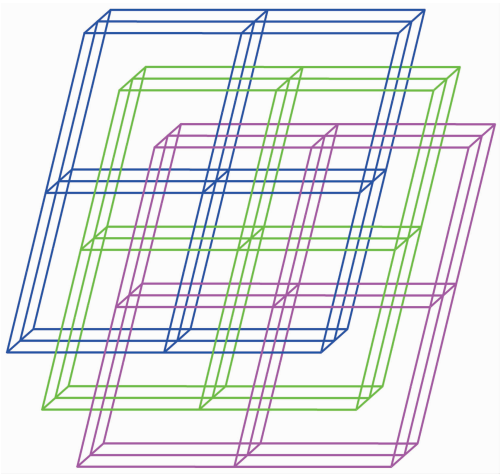

Fig.6　Schematic representation of three-fold interpenetrating 3D α-Po net of **1**

2.2　Crystal structure of 2

When $Co(NO_3)_2\cdot6H_2O$, instead of CdI_2, was used in the reaction of **1**, **2** with a different structure was isolated. Compound **2** crystallizes in the monoclinic space group $P2_1/c$. As shown in Fig.7, there are three kinds of mononuclear molecules consisting of one and two halves of crystallographically unique Co(Ⅱ) ions, four L_1^- ligands, and eight coordinated water molecules in the asymmetric unit. The Co1 ion in **2** is located at a slightly distorted octahedral centre relating two N-bonded L_1^- ligands and four coordinated water molecules, forming a mononuclear molecule of $[Co1(L_1)_2(H_2O)_4]$ while both of Co2 and Co3 ions are sitting on the inversion centers and have octahedral coordination geometry defined by four oxygen atoms from four different water ligands and two nitrogen donors from two different L_1^- ligands. The Co-N (0.210 3(3)~0.214 5(2) nm) and Co-O (0.206 99(19)~0.212 74(19) nm) distances are within the ranges observed for other octahedral complexes[15]. The bond angles around the cobalt ion range from 86.61(8)° to 180.00(1)° (Table 2). The uncoordinated carboxylate groups of HL_1 are deprotonated to act as anionic components to balance the positive charges of the metal ions. Meanwhile, the carboxylate moieties serving as a hydrogen bonding acceptor can effectively benefit the construction of supramolecular structures. As a result, abundant hydrogen bonds are present between terminal coordinated water molecules and carboxylate groups,

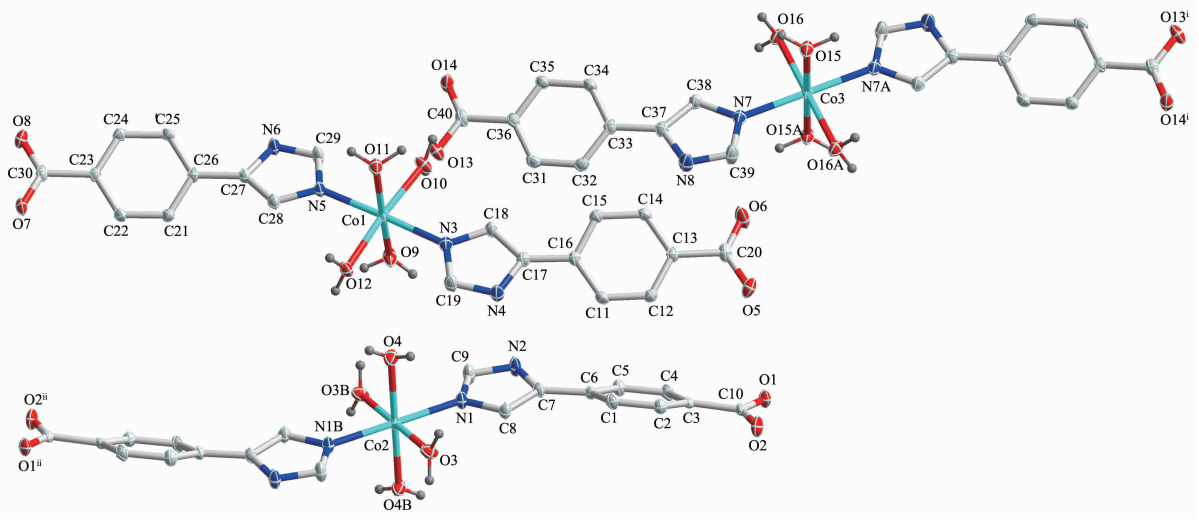

Symmetry code: ⁱ 1−*x*, 1−*y*, 1−*z*; ⁱⁱ −*x*, −*y*, −*z*

Fig.7　View of the coordination environment of Co(Ⅱ) atom with thermal ellipsoids drawn at the 30% probability level for the complex **2**

as exhibited in Table 3. Three kinds of mononuclear molecules are stacked into two-dimensional (2D) layers by hydrogen bonding interactions (N(2)···O(7)^{i} 0.294 2(3) nm, N(2)–H(2A)···O(7) 145.00°; O(3)···O(5)^{ii} 0.261 9(3) nm, O(3)–H(3)···O(5) 151.00°; N(6)···O(14)^{v} 0.279 2(3) nm, N(6)–H(6)···O(14) 146.00°; O(10)···O(13) 0.262 4(3) nm, O(10)–H(10)···O(13) 149.00°; O(12)···O(1)^{iv} 0.272 4(3) nm, O(12)–H(12A)···O(1) 142.00°; O(16)···O(8)^{v} 0.277 7(3) nm, O(16)–H(16)···O(8) 145.00°) along b axis (Table 3, Fig.8). It should be noteworthy that the coordinated water molecules occupy the voids between 2D layers, which contributes to the stabilization of crystal packing of the adjacent 2D layer, further forming 3D supramolecular polymer by hydrogen bonding interactions (Fig.9). For the overall framework of **2**, it can be seen clearly that the three different kind of mononuclear molecules stack sequence into 3D supramolecular polymer along the b axis by rich N–H···O, C–H···O and O–H···O hydrogen bonds interactions.

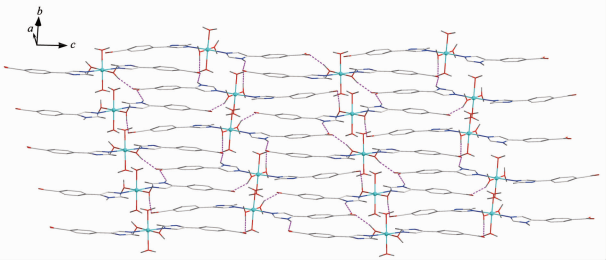

Fig.8 2D layer of **2** linked by hydrogen bonds indicated by dashed line

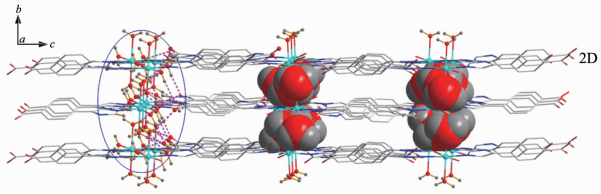

Fig.9 3D supramolecular framework of **2** linked by hydrogen bonds indicated by dashed line (water molecules occupy the voids between the 2D layers highlighted in space-filling)

2.3 Thermal stabilities, powder X-ray diffraction

Complexes **1** and **2** were subjected to thermogravimetric analysis (TGA) to ascertain the stability of supramolecular architecture, and the result is shown in Fig.10. No obvious weight loss was found for **1** before the decomposition of the framework occurred at about 330 ℃, which are in good agreement with the results of the crystal structure. Complex **2** shows a weight loss of 14.04% in the temperature range of 60~175 ℃ corresponding to the release of free water molecules (Calcd. 14.25%) and the decomposition of the residue occurred at 350 ℃. Powder XRD experiment was carried out to confirm the phase purity of bulk sample, and the experimental pattern of the as-synthesized sample can be considered comparable to the corresponding simulated one, indicating the phase purity of the sample (Fig. 11). It should be noted that but the experimental PXRD pattern of desolvated host framework **2′** prepared by drying **2** at 180 ℃ for 24 hours is identical to that of the as-synthesized sample, suggesting that **2′** retains its framework as **2**.

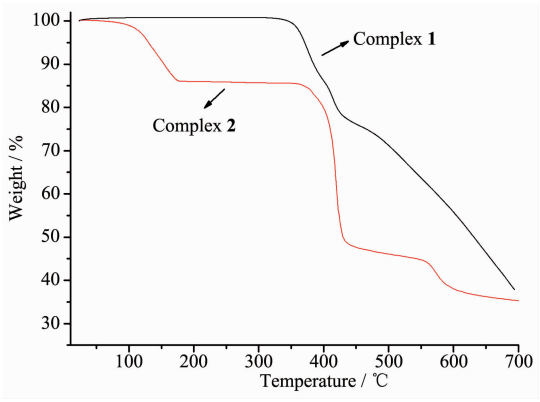

Fig.10 TG curves of **1** and **2**

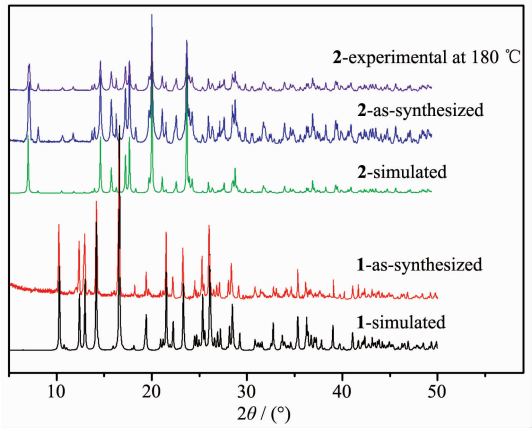

Fig.11 Simulated and experimental PXRD patterns of **1** and **2**

2.4 Spectral properties

The infrared spectrum of the complex has been

recorded between 4 000 and 450 cm^{-1} and some important assignments are shown in the experimental section. The IR spectra exhibit strong absorption centered at 2 639~3 511 cm^{-1} for **1** and **2**, corresponding to the N-H/O-H stretching vibration of ligand or water molecule (see experimental section)[16]. Strong characteristic bands of carboxylic group are observed in the range of 1 570~1 632 cm^{-1} for asymmetric vibrations and 1 411~1 501 cm^{-1} for symmetric vibrations, respectively. The undeprotonation of HL_1 in **1** is also confirmed by the IR spectral data of **1** since a strong band at 1 705 cm^{-1} from -COOH was observed (see Experimental Section)[17].

Compounds constructed by d^{10} metal centers and conjugated organic linkers are promising candidates for photoactive materials with potential applications such as chemical sensors and photochemistry[18]. In this paper, the solid-state photoluminescent property of complex **1** has been investigated as well as free HL_1 ligands in the solid state at room temperature. The free HL_1 ligand shows blue photoluminescence emission at 415 nm upon excitation at 368 nm, which is probably attributable to the $\pi^* \rightarrow n$ or $\pi^* \rightarrow \pi$ transitions, respectively[19-20], while complex **1** exhibits light blue emission with maximum at 438 nm upon excitation at 365 nm as depicted in Fig.12. In contrast to the case for free ligand, the emission bands of complex **1** may be tentatively assigned to intraligand fluorescence since the free ligand exhibit a similar emission under the same condition[21].

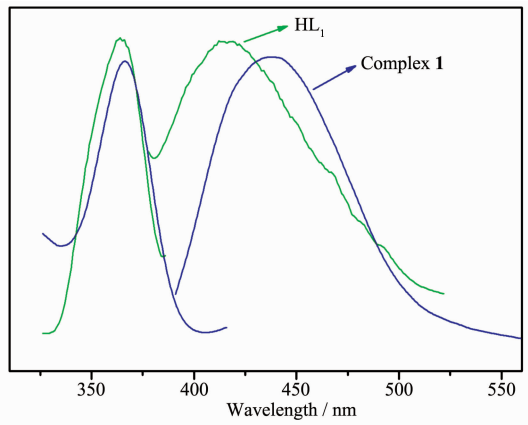

Fig.12　Excitation (left) and emission (right) spectra of complex **1** and the HL_1 ligand

2.5　Sorption property of complex 2

The results of structural analyses show that rich coordinated water molecules occupy the voids between 2D layers in the complex **2** as shown in Fig.9. And TGA and PXRD measurements have been carried out to ascertain the thermal stability of the complex for sorption property investigation, and it was found that the water molecules in **2** can be removed completely by heating to give dehydrated samples of **2′**, without destroying the structure (Fig.11). Therefore, sorption experiments were carried out for the dehydrated samples of **2′**, and adsorption profiles were shown in Fig.13. It is clear that no adsorption of N_2 at 77 K was observed. The H_2O vapor adsorption isotherm at 298 K of **2′** shows rapid uptake in the pressure region of 0~25 kPa and then gradually increase. The final value of the H_2O uptake at 101 kPa is 192.75 $cm^3 \cdot g^{-1}$, corresponding to 3.73 H_2O molecules per formula unit. It is close to the calculated value of 4.0 H_2O molecules indicated by crystallographic analysis. The desorption isotherm does not fit well with the adsorption one and there is a large hysteresis loop with incomplete desorption which may be ascribed to the interactions between the water molecules and the framework as well as the hydrogen bonds between the water molecules[22].

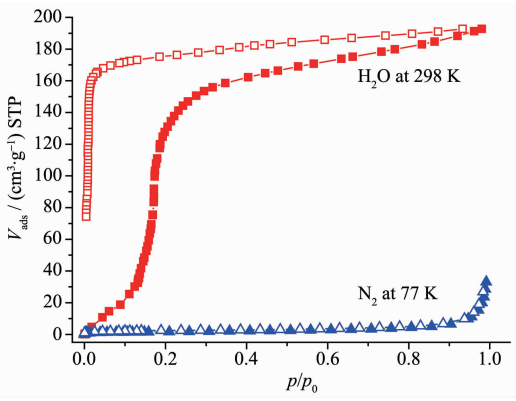

Fig.13　N_2 and H_2O sorption isotherms at 77 and 298 K for **2**: filled shape, adsorption; open shape, desorption

References:

[1] Chen S S, Liu Q, Zhao Y, et al. *Cryst. Growth Des.*, **2014**,

14:3727-3741

[2] MA Zhi-Feng(马志峰), ZHANG Ying-Hui(章应辉), HU Tong-Liang(胡同亮), et al. *Chinese J. Inorg. Chem.*(无机化学学报), **2014**,**30**(1):204-212

[3] ZHAO Yue(赵越), ZHAI Ling-Ling(翟玲玲), SUN Wei-Yin(孙为银). *Chinese J. Inorg. Chem.*(无机化学学报), **2014**,**30**(1):99-105

[4] BAI Zheng-Shuai(白正帅), CHEN Shui-Sheng(陈水生), ZHANG Zheng-Hua(张正华), et al. *Sci. China Ser. B Chem.*(中国科学:化学), **2009**,**52**(4):459-464

[5] Su Z, Chen M, Okamura T, et al. *Inorg. Chem.*, **2011**,**50**:985-991

[6] Chen M, Chen S S, Okamura T, et al. *Cryst. Growth Des.*, **2011**,**11**:1901-1912

[7] CHEN Shui-Sheng(陈水生), ZHANG Shu-Ping(张淑萍), YANG Song(杨松), et al. *Chinese J. Inorg. Chem.*(无机化学学报), **2009**,**25**(6):1000-1004

[8] HU Chun-Yan(胡春燕), XIAO Wei(肖伟), TAO Bai-Long(陶白龙), et al. *Chinese J. Inorg. Chem.*(无机化学学报), **2014**,**30**(2):257-263

[9] Wang L C, Sun J L, Huang Z T, et al. *Cryst. Growth Des.*, **2013**,**13**:1-5

[10]Chen S S, Zhao Y, Fan J, et al. *CrystEngComm*, **2012**,**14**:3564-3576

[11]Chen S S, Chen M, Takamizawa S, et al. *Chem. Commun.*, **2011**,**47**:752-754

[12]*Bruker* 2000, *SMART Version* 5.0, *SAINT-plus Version* 6, *SHELXTL Version* 6.1, *SADABS Version* 2.03. Bruker AXS Inc.: Madison, WI, **2000**.

[13]Du M, Li C. P, Zhao X. J, et al. *CrystEngComm*, **2007**,**9**:1011-1028

[14]Chen S S, Fan J, Okamura T. A, et al. *Cryst. Growth Des.*, **2010**,**10**:812-822

[15]Ma T, Li M X, Wang Z X, et al. *Cryst. Growth Des.*, **2014**,**14**:4155-4165

[16]Nakamoto K. *Infrared and Raman Spectra of Inorganic and Coordinated Compounds*, *5th Ed*. New York: Wiley & Sons, **1997**.

[17]Chen S S, Qiao R, Sheng L Q, et al. *Z. Anorg. Allg. Chem.*, **2013**,**639**:1808-1814

[18]Lu J, Li Y, Zhao K, et al. *Inorg. Chem. Commun.*, **2004**,**7**:1154-1156

[19]Wang X, Qin C, Wang E, et al. *Inorg. Chem.*, **2004**,**43**:1850-1856

[20]Lyons E M, Braverman M A, Supkowski R M, et al. *Inorg. Chem. Commun.*, **2008**,**11**:855-858

[21]Wu G, Wang X F, Okamura T A, et al. *Inorg. Chem.*, **2006**,**45**:8523-8532

[22]Luo L, Wang P, Xu G C, et al. *Cryst. Growth Des.*, **2012**,**12**:2634-2645